### Title

Simultaneous Measurements of Molecular Forces and Electro-Optical Properties of a Confined 5CB Liquid Crystal Film Using a Surface Forces Apparatus




### Journal

Langmuir, 31(13)

### ISSN

0743-7463



### Authors

Kristiansen, Kai
Zeng, Hongbo
Zappone, Bruno
et al.



### Publication Date

2015-04-07

### DOI

10.1021/acs.langmuir.5b00144

Langmuir

Article

pubs.acs.org/Langmuir

# Simultaneous Measurements of Molecular Forces and Electro-Optical Properties of a Confined 5CB Liquid Crystal Film Using a Surface Forces Apparatus

Kai Kristiansen,[†] Hongbo Zeng,[§] Bruno Zappone,[∥] and Jacob N. Israelachvili*[,†,‡]

[†]Department of Chemical Engineering and [‡]Materials Department, University of California, Santa Barbara, Santa Barbara, California 93106, United States

[§]Department of Chemical and Materials Engineering, University of Alberta, Edmonton, AB T6G 2V4, Canada

[∥]Consiglio Nazionale delle Ricerche, Istituto di Nanotecnologia (CNR-Nanotech) Unità di Cosenza, LICRYL c/o Dipartimento di Fisica, Università della Calabria , Cubo 33/B, 87036 Rende (CS), Italy

Supporting Information

**ABSTRACT:** Using a surface forces apparatus (SFA), we studied the forces associated with the reorientation of molecules of a common nematic thermotropic liquid crystal, 4′-*n*-pentyl-4-cyanobiphenyl (5CB), confined between two conducting (silver) surfaces and its optical behavior under the influence of electric fields with varying magnitudes and field directions. A transient attractive force was observed due to partial reorientations of the liquid crystal molecules and the flow of free ions, in addition to a stronger constant capacitance attraction between the silver surfaces. At the same time, the optical properties of the liquid crystals were observed perpendicular to the silver surfaces. Observations of shifts and fluctuations of the extraordinary wave of the (multiple beam) interference fringes measure the refractive index of the director component parallel to the surface, which is sensitive to tilt motion (or reorientation) of the liquid crystal molecules that provided details of the anisotropic orientations of the molecules and domains. Any lateral differential refractive index change is easily observed by optical microscopy. The optical microscope imaging showed that the changes in the optical properties are due to convective flow at domain boundaries of the liquid crystal molecules (and possible free ions) between the two charged surfaces. At low electric fields, propagation of domain boundaries was observed, while at higher electric fields, hexagonal patterns of flowing molecules were observed. The interplay of the force measurements and optical observations reveal a complex dynamic behavior of liquid crystals subjected to varying electric fields in confined spaces.

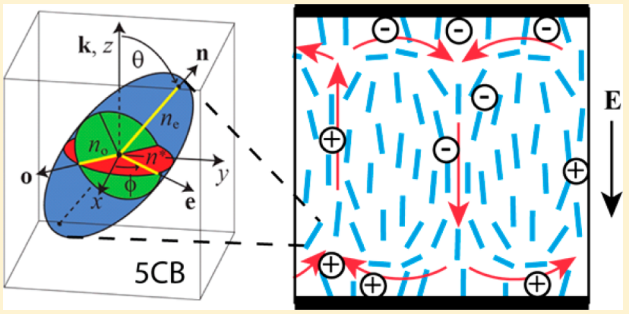


## INTRODUCTION

Nematic liquid crystals are fluid materials with long-range orientational order. Their anisotropic optical properties can easily be manipulated by external electric, magnetic, and electromagnetic fields, which have been utilized in applications including display devices and beyond.[1,2] The natural state of liquid crystal molecules, which contain an intrinsic electrical dipole moment, is in a dimer configuration. It is believed that such liquid crystals interact with an external electric field through the polarizability of domains (cluster of multiple molecules) as a whole rather than with the individual dipole moment of each molecule.[3] The liquid crystals exhibit a multitude of behaviors from electro-optical response, collective reorientation via domain formation,[4] and complex flow patterns depending on the strength and orientation of these external electric and magnetic fields[5] as well as anchoring to the surface. The behavior of the liquid crystals also depends on the presence of free ions (similar to free ions present in ionic liquids[6]), where the formation of free ions is temperature dependent.

Because of its technological and industrial importance, the emphasis on liquid crystal research is on the optical response in an electric field and not as focused on the forces exhibited by the liquid crystal in an electric field. Here we use a surface forces apparatus (SFA) to study the forces that a liquid crystal experiences and exerts in electric fields. The separation distance, *D*, between the two electrode surfaces in this study was chosen to be similar to that in liquid crystal displays (LCD). In a first approximation, the critical voltages of the Freedericksz transition and onset of hydrodynamic instability are independent of the separation distance, *D* (see below), but surface effects like electrostatic and steric repulsion have been

**Received:** January 21, 2015
**Revised:** March 13, 2015
**Published:** March 16, 2015



  

DOI: 10.1021/acs.langmuir.5b00144
*Langmuir* 2015, 31, 3965−3972

observed below 300 nm.[7−9] However, these surface effects are beyond the scope of this study.

Several methods exist for measuring properties of a nematic liquid crystal using optical techniques[10−12] and force sensing techniques.[13] The surface forces apparatus (SFA) is a technique that accurately uses both techniques to measure thin films in general[14] and liquid crystal in particular.[7,15] Recently the SFA has been used to study surface forces and concurrently the thin film patterns induced by an external electric field.[16] Here we want to monitor in real time the formation of domains and the refractive index changes using two optical techniques: direct optical microscope visualization and multiple-beam interferometry employing fringes of equal chromatic order (FECO), respectively. The imaging is accompanied by surface force measurements.

## MATERIALS AND METHODS

**Materials.** The liquid crystal 4′-*n*-pentyl-4-cyanobiphenyl (5CB) was purchased (98% purity assay) from Sigma-Aldrich and used as received. All experiments are performed at room temperature (23 °C), and at this temperature the 5CB is in a nematic phase. A small volume (100 $\mu$L) of 5CB liquid crystal was injected between two smooth silver surfaces in a surface forces apparatus (SFA2000, SurForce LLC).

**Surface Preparations.** A 55 nm thick layer of silver was thermal evaporated onto a freshly cleaved and atomically smooth mica of thickness 3−5 $\mu$m. The silvered mica (Ag rms roughness of a few nanometers) was glued with EPON 1004, mica side down, onto a cylindrical glass disk. A pair of the cylindrical glass disks (with nominal radius of curvature of 20 mm) with silvered mica was installed in a cross-cylindrical configuration into the SFA. The two silver surfaces were brought together to a minimum Ag−Ag surface gap distance $D$ of 7 $\mu$m, which was used throughout our experiments unless otherwise noted.

**Surface Distance and Refractive Index Measurements.** The two apposing silver surfaces in the SFA serve two purposes (see Figure 1): mirror and electrode. The silver surfaces act as a mirror for the multiple beam interference (MBI) method of the SFA technique.[14] The MBI produces fringes of equal chromatic order (FECO), where the wavelengths of the FECO are read out through a spectrometer and recorded by a camera (MTI SIT VE-1000). The FECO fringes are used for accurate distance and refractive index measurements (measured at the point of closest approach between the surfaces) and for monitoring the profile of the surfaces. The surface separation distance $D$ and the alignement of the 5CB director **n** (Figure 1) were determined using a multiple-beam interferometry technique,[14] discussed below.

The orientation of **n** can be qualitatively observed from a top view of the surfaces and recorded using a camera (Pulnix TM-200).

**Electric Field.** The silver surfaces were also used as the two electrodes. Conductive glue was used to connect a thin electrical wire to each of the two surfaces. The spot of conductive glue was shielded with a layer of UV curing glue (NOA63) in order to minimize potential contamination of the liquid crystal. The surfaces were then connected to a function generator (HP 3325B) that can produce various waveforms over a wide range of frequencies (1 $\mu$Hz to several MHz) and voltages (from 0 to ±20 V). A square-wave with frequency 0.05 Hz was typically applied in the conducted experiments.

**Surface Forces Measurements.** The lateral and normal forces between the surfaces were measured using a 3D actuator−sensor attachment[14] for the SFA2000. The signals from the strain gauges in the 3D actuator−sensor that are laid in a Wheatstone configuration are amplified by a signal conditioning amplifier (Vishay 2311), and the output voltages are read out through a chart recorder (Soltec 1242).

## RESULTS AND DISCUSSION

**Surface Anchoring and Director Orientation.** 5CB is an optically anisotropic, positive uniaxial LC (Figure 2). The optical axis is parallel to director **n** and makes a zenithal (tilt) angle $\theta$ with the wave vector **k**, parallel to the substrate normal $z$. To specify the directions **o** and **e** of the ordinary and extraordinary axis of polarization, respectively, an additional

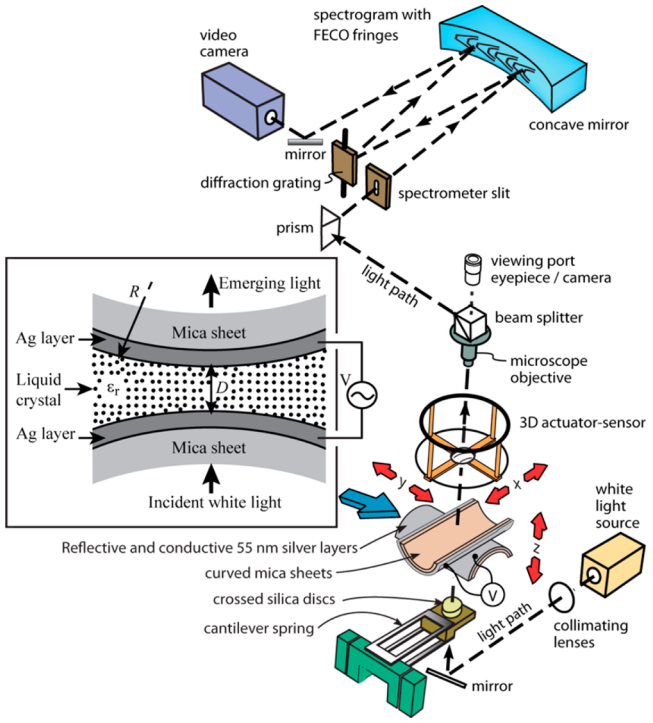


**Figure 1.** Experimental setup. (a) The liquid crystal (5CB) is trapped between two reflecting silver electrodes in a cross-cylinder configuration. The radius of the surfaces is not drawn to scale for illustration purposes; in practice, the surfaces are effectively locally flat over the areas investigated (see Figure 3b for the normal and lateral distance scales). The electrical potential difference between the two electrodes is controlled by a function generator. (b) The lower surface sits on a double-cantilever spring while the upper surface is placed on the 3D actuator−sensor attachment to the SFA2000. White light is passed normal through the electrode surfaces for electrode separation distance determination using a spectrometer and for observing domain formation in the liquid crystal through a top view camera.

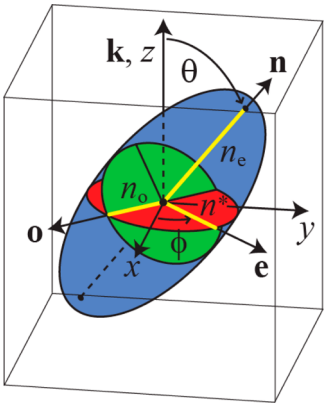


**Figure 2.** 5CB is a optically anisotropic, positive uniaxial material. The optical axis is parallel to director **n** and makes a (zenithal) angle $\theta$ with the wavevector **k**, parallel to the substrate normal $z$. The directions of ordinary (**o**) and extraordinary (**e**) polarization specified by the additional (azimuthal) angle $\phi$. The ordinary refractive index $n_0$ does not depend on $\theta$, as opposed to the extraordinary refractive $n^* < n_e$. The direction $x$ corresponds to the entrance slit of the spectrometer.





DOI: 10.1021/acs.langmuir.5b00144
*Langmuir* 2015, 31, 3965−3972

azimuthal angle $\phi$ is required. The 5CB film was birefringent between crossed polarizers, right after injection of 5CB and without any applied voltage; therefore, the average zenithal angle in the film thickness was $\theta < 90°$. The alignment of **n** was not uniform on the surface and domains could be observed (see Figure 3a).

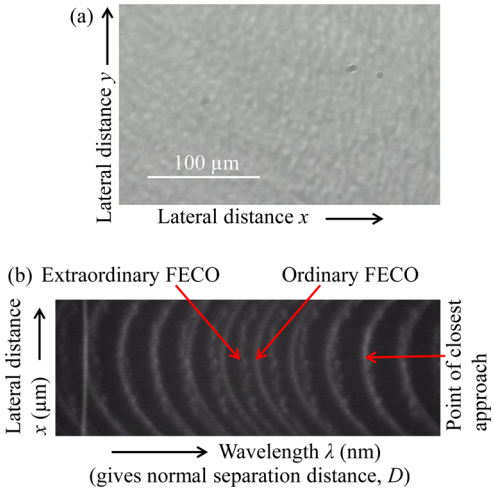


**Figure 3.** Optical images of 5CB film of thickness $D \approx 50$ $\mu$m between two silver surfaces. (a) Optical microscope (no filters) showing domains. (b) Spectrogram showing FECOs produced by MBI between two mirror silver surfaces confining the 5CB film. Smooth and jagged FECOs are generated respectively by ordinary and extraordinary fringes. The horizontal axis is the wavelength while the vertical axis corresponds to a direction $x$ parallel to the mirror surfaces. The parabolic-shaped fringes reflect the curved geometry of the surface along $x$, and the fringe tip is the point of closest approach between the surfaces.

Figure 3b shows a spectrogram obtained when the surfaces were separated by $D \approx 50$ $\mu$m. Two types of fringes of FECOs are visible: smooth and jagged fringes, which appear curved due to the curvature of the mirror surface. To explain such a difference, we consider ordinary and polarized waves undergoing MBI within the 5CB film between the silver mirrors. If $d\phi/dz \ll \Delta n/\lambda$, where $\lambda$ is the wavelength and $\Delta n = (n_e - n_0)$ is the maximum birefringence (Figure 2), the polarization of a wave relative to the local ($z$-dependent) axes **o** and **e** is preserved for all $z$ (Mauguin criterion for adiabatic propagation).[5] In our case, calling $\phi_1$ and $\phi_2$ the angles at the surfaces, we have $(\phi_1 - \phi_2) \leq \pi/2$ and $d\phi/dz = (\phi_1 - \phi_2)/D \leq \pi/2D \ll \Delta n/\lambda$. Therefore, the Mauguin criterion is satisfied, and waves with orthogonal polarization do not interfere with each other. Hence, smooth fringes corresponded to MBI of ordinary waves entering the surfaces at different points in the $xy$-plane and propagating with the same refractive index $n_0$, independent of the zenithal angle $\theta$ (Figure 2).

The condition of resonance for multiple reflections between the silver mirror is $n_0 D = q\lambda_q^0/2$, where $q$ is the chromatic order and $\lambda_q^0$ is the ordinary wavelength that only depends on the ordinary refractive index, $n_0$. Therefore, the distance $D$ can be determined by measuring the wavelength $\lambda_{q-1}^0$ and $\lambda_q^0$ of two consecutive smooth fringes:

$$n_0 D = \frac{\lambda_{q-1}^0 \lambda_q^0}{2(\lambda_{q-1}^0 - \lambda_q^0)} \quad (1)$$

On the other hand, the propagation of extraordinary fringes depends on the local value of $\theta$ that may vary along $z$ and between different points of the $xy$-plane (Figure 1). Jagged fringes correspond to such extraordinary waves propagating with an index $n^*(\theta)$. The jaggedness shows that the angle $\theta$, averaged across the film thickness, varied at different points of the $x$ direction (Figure 3). The average value of $n^*$ was calculated at the point of closest approach (see Figure 3 and schematic in Figure 1) using eq 1 by considering the wavelengths $\lambda_{q-1}^e$ and $\lambda_q^e$ of two consecutive (jagged) extraordinary FECOs. At room temperature (23 °C) the ordinary index of 5CB is $n_0 = 1.53$. The average extraordinary index $n^*$ for the 5CB is given by

$$n^* \approx [(\cos\bar{\theta}/n_e)^2 + (\sin\bar{\theta}/n_0)^2]^{-1/2} \quad (2)$$

where $\bar{\theta}$ is the $z$-averaged zenithal angle and the maximum value $n^* = n_e = 1.72$ is obtained when the director **n** is uniform and parallel to the surfaces ($\theta = 90°$ in Figure 1).[11] In our case, $n^* = 1.68$, corresponding to an average tilt angle $\bar{\theta} \approx 65°$. Therefore, the anchoring of 5CB on silver was close to planar but tilted from the Ag surface.

**Electro-Optical Response.** In the presence of an external electric field, the liquid crystal molecules experience a force trying to align the molecules with their director parallel to the electric field direction. In a uniform, planar film with parallel anchoring ($\theta = 90°$), an abrupt reorientation of the director **n** occurs in the film middle ($z = D/2$) for voltages above a critical value $V_c$, independent from $D$, known as the Freedericksz threshold:[5]

$$V_c = \pi\left[\frac{K_{11}}{\varepsilon_0 \varepsilon_a}\right]^{1/2} = 0.8 \text{ V} \quad (3)$$

where $\varepsilon_0$ is the vacuum permittivity, and $K_{11} = 6.65$ pN (ref 17) and $\varepsilon_a = 11.5$ (ref 18) are the splay elastic constant and dielectric anisotropy of 5CB at 23 °C, respectively.

Any force exerted on the silver surfaces by either the attractive oppositely charged surfaces or induced by the liquid crystal will be measured by the 3D actuator−sensor attachment to the SFA. Here we studied the electric field effect on the refractive index of 5CB. An external square-wave voltage of frequency 0.05 Hz (unless noted) was applied to the system, where the amplitude was varied from 0 to 20 V. In the absence of any external electric field, the FECO patterns (see Figures 3 and 7a) show smooth and jagged fringes, which correspond to the ordinary and extraordinary fringes, respectively.

On applying a voltage $V \geq 0.5$ V, ordinary fringes remain mainly unperturbed while extraordinary fringes move to shorter wavelengths with a wavy motion along the fringes. In Figure 7, panels a and b show how the extraordinary fringes shift after applying 1 V. Since the position of the ordinary fringes vary with the distance $D$ (eq 1) but does not depend on the director orientation (Figure 1), stationary ordinary fringes indicate that the surface did not move while the director was reoriented upon applying the voltage, changing the value of $n^*$ (eq 2). Therefore, the shifting of extraordinary FECOs was due to a field-induced director reorientation that occurred for $V \geq 0.5$ V. The extraordinary fringes did not overlap completely with the ordinary ones (i.e., $n^* > n_0$ in eq 2), indicating that the reorientation of the director **n** along the field (and surface normal) was not complete over the entire film thickness but limited to the film middle, as expected for low voltages.[5]





DOI: 10.1021/acs.langmuir.5b00144
Langmuir 2015, 31, 3965−3972

The minimum voltage of 0.5 V at which we observed a reorientation was slightly lower than the critical voltage $V_c$ (eq 3). In our case, however, the anchoring direction was tilted from the Ag substrate, and the Freedericksz transition is expected to be less sharp, with a small reorientation of **n** in the film middle already for voltages smaller than but close to critical voltage $V_c$.[19] Also, the confinement geometry of the SFA is that of a sphere and a plane, which distorts the director even for $V$ = 0 and induces a splay deformation in the **n** field.

In the voltage range between 0.5 and 5 V, an abrupt reversal of voltage polarity induces a shift in the extraordinary fringes to shorter wavelengths, without measurable variations of the surface distance $D$. Figure 7c shows the shift going from +1 to −1 V, while Figure 7d shows that the extraordinary fringe relaxes back to the position close to where it was before the polarity reversal, as expected. The time span for the fringe to come back to this position is about 1 s. An asymmetry of the wavelength shift was often observed dependent on the direction of the polarity reversal (see Figure 7). Moreover, over the course of many reversal cycles, the extraordinary fringe approaches and overlaps the ordinary fringe without relaxing back.

Video SV1 in the Supporting Information shows the FECO fringes of 5CB under an electric field induced by a square-wave voltage of 2.0 V and frequency 0.05 Hz. The extraordinary fringes show a wavy motion along the lateral direction, indicating undulating domains. These undulating domains can also be observed through an optical microscope (top view of surfaces, see Figure 1 and Video SV2 in the Supporting Information). The asymmetry of the wavelength shift is also seen in Video SV1.

At higher voltages (>5 V) the extraordinary wave overlaps with the ordinary after a few polarity reversals. This indicates that the 5CB film tends to become less birefringent as the number of cycle increases; i.e., the director tends to align normal to the surfaces reducing the difference between $n_0$ and $n^*$. Most likely, the silver surfaces are degrading over time as the cyano groups in the 5CB molecules react with the silver surfaces. The reaction rate is increased by the applied voltage (the measurements at 20 V only last a few minutes before significant damage occurs on the silver surface). The degrading of the silver surfaces also results in diminishing of the brightness of the FECO fringes. However, the degrading of the silver surfaces was found not to affect the forces (see below) and therefore does not give rise to additional free ions or ionic impurities.

**Force Measurements.** Figure 4 shows a typical experiment where a square-wave voltage is applied between the two silver surface separated by a thin film of 5CB and the corresponding normal force is measured. No lateral forces were detected in all of the measurements. After applying the electric field (voltage potential difference from 0 to $V$ between Ag surfaces), the electrostatic "capacitance" attraction between the two silver surfaces was immediately measured by the sensor in the direction normal to the surfaces. The initial electrostatic attractive force $F_E$ between the two electrodes at constant potential $V$ is given by the equation for sphere on flat capacitor:[20]

$$F_E = \frac{\pi \varepsilon_{zz}(\theta)\varepsilon_0 R V^2}{D} \quad (4)$$

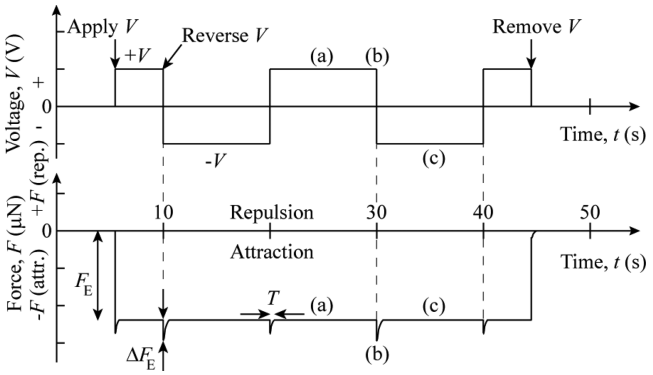


**Figure 4.** Typical measured force between two electrode surfaces separated by a thin layer of liquid crystals (5CB) in a square-wave varying electrical potential difference (i.e., applied voltage). The square-wave electrical potential difference (upper panel) was applied across the two electrodes (Ag surfaces) during the experiments resulting in (lower panel) an attractive force curve (e.g., points a and c) with additional attractive transient force at the point when the applied voltage reverses polarity (at point b).

where $D$ is the distance between the two electrodes (see eq 1), $\varepsilon_0 = 8.85 \times 10^{-12}$ F/m is the permittivity in vacuum, $R$ is the radius of curvature of the sphere-on-flat configuration, and $\varepsilon_{zz}(\theta) = \varepsilon_\perp + \varepsilon_a \cos^2 \theta$ is the dielectric constant for an electric field oriented along the surface normal $z$ at stationary (zero frequency) conditions; alternatively, we could use $\varepsilon_{zz} = \varepsilon_{zz}(V/V_c)$ instead of $\varepsilon_{zz} = \varepsilon_{zz}(\theta)$. The director is at an angle $\theta$ from the $z$-axis and $\varepsilon_a = \varepsilon_\parallel - \varepsilon_\perp$ is the dielectric anisotropy, i.e., the difference between the dielectric constant parallel to the director $\varepsilon_\parallel$ and perpendicular to the director $\varepsilon_\perp$.

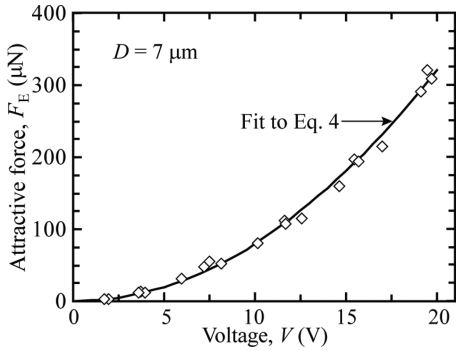


**Figure 5.** (a) Electrostatic force between two electrodes fits well to the parabolic equation of a parallel capacitor plate, eq 4. A power law fit to the experimental point gives a slope of 2.05 ± 0.03, which within uncertainty is similar to the theoretical value of 2.

Figure 5 shows how the initial attractive force $F_E$ increases with the magnitude of the applied voltage $V$. The solid line is a fit to the experimental data, and it shows a power law dependence of $F_E$ with $V$, with a power of magnitude 2.05 ± 0.03, which is close to the predicted value of 2 in eq 4. The best fit to the data of Figure 5 and eq 4 (with $D$ = 7.0 $\mu$m, $R$ = 20 mm) gives $\varepsilon_{zz}(\theta)$ = 10.1 ± 0.3, which is between the literature values[18] of dielectric constants parallel, $\varepsilon_\parallel$ = 19.5, and perpendicular, $\varepsilon_\perp$ = 6.5, to the director. With the measured value of $\varepsilon_{zz}(\theta)$ = 10.1, then the director is at an angle $\theta$ = 58° away from the surface normal. This is close to the value obtained for $V$ = 0 (about 65°).



DOI: 10.1021/acs.langmuir.5b00144
Langmuir 2015, 31, 3965−3972

There is an additional attractive force, $\Delta F_E$, along with the capacitor force when the voltage changes polarity (Figure 4b) and when the magnitude is $V \geq 0.5$ V. During the voltage reversal, the change in the separation distance $D$ and the radius of curvature $R$ is negligible. $\Delta F_E$ decays in less than a second and corresponds to the relaxation of the extraordinary fringes following the polarity reversal (Figure 7a–d). One of the major contributions to $\Delta F_E$ stems from the transient change in the dielectric constant $\Delta\varepsilon_{zz} = \varepsilon_a \Delta \cos^2\theta$ due to change in director orientation:

$$\Delta F_E = \frac{\pi \Delta\varepsilon_{zz}(\theta)\varepsilon_0 R V^2}{D} \quad (5)$$

Charging of the surfaces or anchoring of 5CB on the surfaces can lead to a small asymmetry of the system.[8] Even a small amount of adsorbed free ions on one of the surfaces can have a dramatic effect on the anchoring properties.[21] The asymmetry manifests itself through the observation of alternating strong and weak responses to the change in the direction of the electric field. Figure 6 shows the additional force $\Delta F_E$ as a function of the applied voltage, and we find $\Delta\varepsilon_{zz,low} = 1.2 \pm 0.2$ and $\Delta\varepsilon_{zz,high} = 1.8 \pm 0.2$. With the average measured value of $\Delta\varepsilon_{zz}(\theta) = 1.5$, then the director is at an angle $\theta = 51°$ away from the surface normal. A rough estimate indicates that 10% of the total number of 5CB molecules in the droplet contributes to the refractive index change (see eq S1 in the Supporting Information).

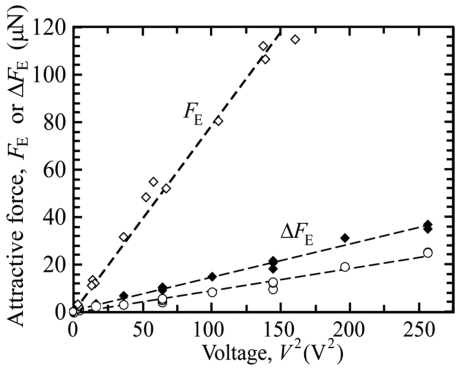


**Figure 6.** Measured attractive "rotation" force $\Delta F_E$ when the two silver electrodes reverse polarity and compared to the capacitor force $F_E$. The $\Delta F_E$ is observed at voltages greater than 0.5 V, and it increases as the square of the voltage (see eq 5). The asymmetry of $\Delta F_E$, which depends on the polarity of the applied voltage (solid diamonds are the forces measured on reversing $V$ at a polarity different from the open circles), is caused by surface effects like anchoring of liquid crystal molecules and asymmetric adsorption of free ions on the surface (see main text).

$\Delta F_E$ cannot be due only to a change in the dielectric constant $\varepsilon_{zz}$ in eq 5 associated with reorientation, which occurs on a short time scale of 10 ms. Another major contributor to $\Delta F_E$ is free ions in 5CB that move faster along the director **n** than along other directions in response to an external field. In an external field $E_0$, **n** is reoriented toward the normal $z$ to the electrodes and ions are induces to flow toward the oppositely charged electrodes (some charges may be shuttled on "cargo" particles[22]), which builds up an internal field $E_i$ in direction opposite to $E_0$. The internal field reaches a saturation value after a characteristic relaxation time $\tau \propto D^2/(V - V_c)$, where $V_c$ is the threshold voltage for the Freedericksz transition and $D$ is

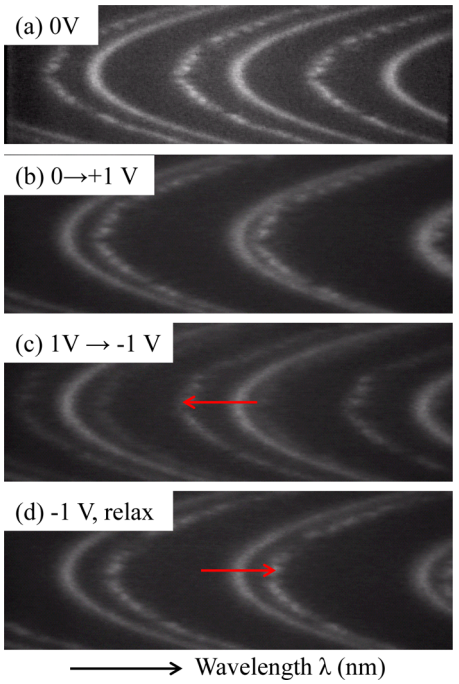


**Figure 7.** Shift of the wavelength of extraordinary FECO fringes as the potential drops over the 5 CB changes from no voltage to +1 V and then reverses to −1 V. (a) Before any applied voltage we see a splitting of the FECO fringes. (b) After applying 1 V the extraordinary FECO fringe move to shorter wavelengths, toward the ordinary fringes, over several fields of view in less than 1 s. (c, d) When the polarity of the voltage reverses, the extraordinary fringe moves to lower wavelengths before it relaxes back within a second. The average extraordinary index at 1 V (relaxed state) is here $n^* = 1.66$ and at 1 V (at polarity shift) $n^* = 1.64$, which correspond to (eq 2) average tilt angles of 59° and 52°, respectively (close to the average angle of 58° found based on Figure 5).

the surface separation (for numerical values of $\tau$, see eq 16 in ref 23). We estimate the relaxation time to be $\tau \approx 1$ s for the separation $D = 7$ $\mu$m considered in the present work, in agreement with the observed overshoot time. Therefore, the overshoot $\Delta F_E$ is due to the progressive decay of the total field $E = E_0 - E_i$ in the 5CB film and electrostatic force $F_E$ in eq 4. This mechanism also explains the abrupt shift of the extraordinary fringes toward *lower* wavelengths at the time $t_0$ of the polarity reversal. Until the ionic drift toward the oppositely charged electrode is complete, the ions face the electrode with the same charge. Therefore, during the time between $t_0$ and $t_0 + \tau$ the total field is $E_0 + E_i$ and the director is reoriented by a stronger field, and $n^*$ is closer to $n_0$ in eq 4 than at times $t > t_0 + \tau$. The electrostatic force $F_E$ is also stronger at time $t_0$ because the dielectric constant $\varepsilon_{zz}$ in eq 4 is closer to the maximum value $\varepsilon_{||} = 19.5$ than at later times. Also notice that $\Delta F_E$ is higher for the first polarity reversal in Figure 4b than at the time when the field is reversed on for the first time. This may also be explained considering that the field is $E_0$ at switch-on time and $E_0 + E_i$ at the first polarity reversal.

The phase of a liquid crystal (as 5CB) changes with the temperature, and $\Delta F_E$ is found to vary with temperature. At 16 °C (crystalline phase) the magnitude of $\Delta F_E$ is reduced to about half compared to the measurements at 23 °C. The reduced magnitude of $\Delta F_E$ is related to the reduction of the mole fraction of free ions $X_{free}$ in the liquid crystal solution. Similar to ionic liquids,[6] we can assume in a first approximation





DOI: 10.1021/acs.langmuir.5b00144
*Langmuir* 2015, 31, 3965−3972

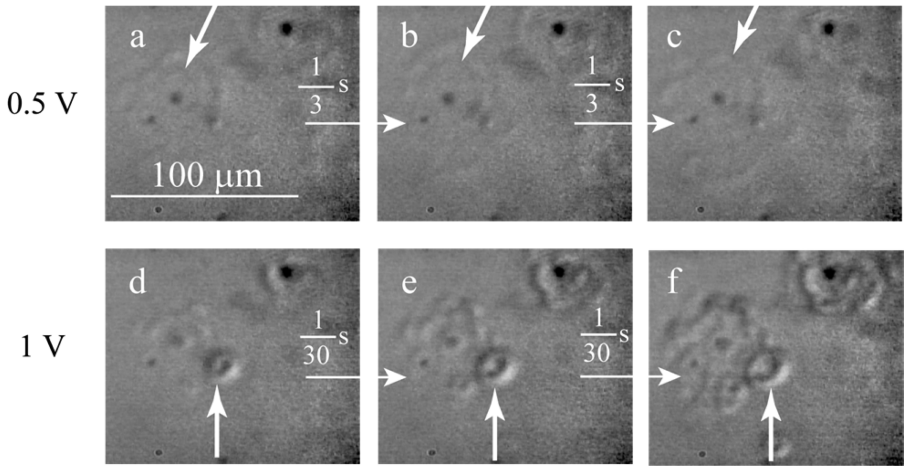


**Figure 8.** Velocity of the propagation of the domains' boundary of the liquid crystals determined from the top view (i.e., microscope view). The white arrow on each picture points to a domain boundary that is expanding radially outward. The sequence (a → c) shows the evolution of one domain boundary at 0.5 V over 2/3 of a second. The sequence (d → f) shows the evolution of one domain boundary at 1 V over 2/30 of a second. The velocity of the domains from the sequences at 0.5 and 1 V is found to be 20 ± 5 $\mu$m/s.

that $X_{free}$ follows a Boltzmann distribution: $X_{free} \approx \exp[-E_d/(\varepsilon kT)]$, where $E_d$ is the ion dissociation energy in vacuum and $k$ is Boltzmann's constant. The crystalline phase hinders the molecules' rotation, and fewer molecules participate in the rotation force, which leads to a smaller magnitude of the $\Delta F_E$. At 44 °C (isotropic phase) no additional attraction force is observed. The isotropic phase does not possess the long-ranged order of the liquid crystal molecules, which indicates that collective motion is necessary for the rotation force and that free ions are less important in the rotation force.

The attractive force $\Delta F_E$ is also limited by the orientational relaxation time of the confined liquid crystal. Changing the frequency of the square-wave signal from 0.01 to 1 Hz reveals that $\Delta F_E$ is constant up to 0.7 Hz, where above 0.7 Hz the attractive force starts to decrease. This frequency corresponds to the relaxation time after the overshoot, as seen in the schematic of the attractive force-time profile in Figure 4.

**Flow Patterns Observed from Optical Microscopy.** Above a critical voltage, ionic elements and free ions in the liquid crystal induce a flow pattern or a Carr−Helfrich mode of electrohydrodynamic instability.[1] These flow patterns can easily be observed using optical microscopy as the director of the liquid crystal fluctuates at the boundaries of the undulating flow patterns (see Video SV2 in the Supporting Information). Figure 8 shows how these flow patterns form circular domains and propagate at low voltage between 0.5 and 1.0 V. The speed of propagation of the boundaries is 20 $\mu$m/s for both 0.5 and 1.0 V. The critical voltage for electrohydrodynamic instability in thin nematic liquid crystals has been previously found to be of the order of a few volts.[1]

At voltages above 1.5 V, Figure 9 shows that the fluctuating boundaries appear more readily. The close packing guides the pattern of the boundaries to form hexagonal-shaped domains. The size distribution of the domains appears broad in the voltage region between 1.5 and 5 V, while above 5 V the domains form close to a regular lattice of hexagons. Figure 10 shows a schematic of the possible behavior of the liquid crystal in electric fields. At high voltage, a Carr−Helfrich mode of electrohydrodynamic instability formed from moving ionic elements and free ions in the liquid crystal. These charged entities are transported from one surface to the other and cause the liquid crystal molecule nearby to fluctuate. These

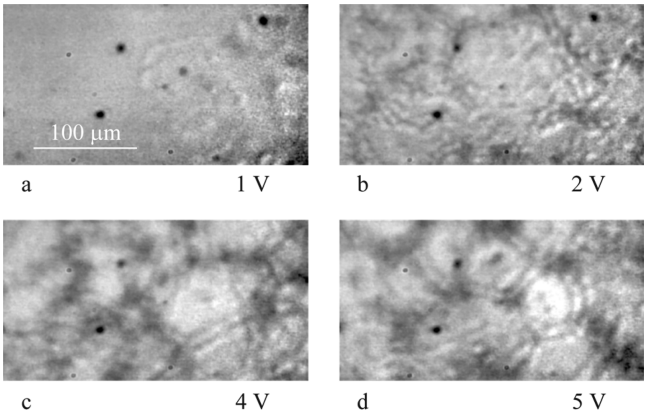


**Figure 9.** Qualitative description of the development of the nucleation sites and boundary propagation of liquid crystals in electric fields of various strength. At low electric field (a, b) the boundary nucleates and propagates in expanding circular rings. (b−d) With applied voltage higher than 1 V, all the area of liquid crystal is covered by fluctuating and propagating boundaries. The domains of fluctuating boundaries are apparently separated from the rest of the liquid crystal. From 1.5−3 V the domains are large; thus, the boundaries can propagate over long distance. In this region the shape of the domains turns from circular to hexagon due to close packing. From 3 to 5 V the domains get more separated (or defined) and break up to smaller units. At 5 V some of the domains merge, and they form a more regular lattice of clearly separated hexagon domains. Figure S1 shows the same images with the domain boundaries indicated by white circles and hexagons.

fluctuations of the optical anisotropic liquid crystal molecules are seen by optical microscope as a boundary. The lower panel of Figure 10 shows that a continuous flow pattern (with neither sink nor source) is possible.

Immediately after the voltage reversal, the top view of the sample reveals that the liquid crystal appears uniform; i.e., the film of liquid crystal has the same refractive index throughout the plane. Shortly after the voltage reversal, domains start forming again, which indicate that the refractive index is nonuniform throughout the sample (see Video SV2 in the Supporting Information). The transition from domains to uniform film to domains again coincides with the observed attractive force $\Delta F_E$.




DOI: 10.1021/acs.langmuir.5b00144
Langmuir 2015, 31, 3965−3972

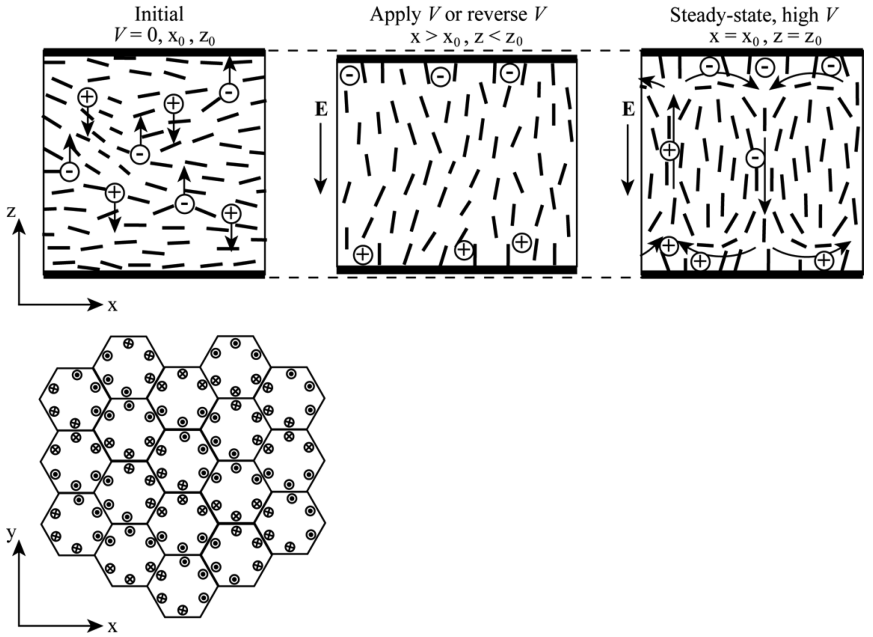


**Figure 10.** Schematic of possible responses of a liquid crystal to an external electric field. The top panel shows the side view of the liquid crystals. Initially, the liquid crystal molecules are ordered and parallel to the surfaces, and free ions are randomly distributed throughout the solution. Applying a voltage between the surfaces (external electric field) or reversing the polarity of the voltage causes an attractive force between the surfaces. The liquid crystal molecules tend to align with the electric field, and the free ions flow to the oppositely charged surface. At high voltage, flow patterns in hexagonal lattice arrangement is observed, where the liquid crystals are fluctuating at the domain boundaries and the free ions are transferred to the other surface at the boundaries. The lower panel shows a possible hexagonal flow pattern, where the arrowhead means flow goes out of the plane, while the arrow tail means flow goes into the plane.

## CONCLUSIONS

Force measurements using an SFA with multiple-beam interference optical imaging together with simultaneous microscope imaging reveal a rich and complex behavior of confined nematic liquid crystals under external electric fields and especially when the polarity of the voltage on the surfaces is abruptly reversed. Observations of shifts and fluctuations of the extraordinary wave of the (multiple beam) interference fringes measure the refractive index of the director component parallel to the surface, which is sensitive to tilt motion (or reorientation) of the liquid crystal molecules that provided details of the anisotropic orientations of the molecules and domains. Any lateral differential refractive index change was easily observed by optic microscopy.

The two electrode surfaces display an attractive force that varies with the voltage, as described by the regular capacitor equation, and scales with an effective dielectric constant of the liquid crystal trapped between them. Below the Freedericksz transition (in this study about 0.5 V), no transient force was detected and no change in the refractive index was observed when the polarity of the voltage was reversed. Above the Freedericksz transition, an additional transient attractive force (in addition to the capacitor force) is observed when the polarity of the voltage is reversed. This transient force is attributed to rotation of the molecules of the liquid crystal revealed by shifts of the refractive index of the liquid crystal, as well as free ions. Free ions and strong anchoring of the liquid molecules are the likely causes of the observed asymmetry in the rotation force.

A film of liquid crystals forms mobile domains under the influence of a perpendicular electric field. At low voltages a domain is nucleated at a defect within the liquid crystal or at an impurity site and expands until it hits another domain. At higher voltages (>3 V), rapid formation of fluctuating domain boundaries are observed, caused by the anisotropic flow of the liquid crystal molecules and free ions, resulting in close packing of the domains into a hexagonal lattice.

The use of a multimodal SFA, as in the combination used here of electric field, interaction forces, refractive index, and optical microscopy, opens up new methods in the field of liquid crystals research to study the intersection between refractive index shifts of the director within domains of liquid crystal molecules under the influence of an external electric (or magnetic or electromagnetic) field and the corresponding forces these molecules impose on the confining surfaces.

## ASSOCIATED CONTENT

### Supporting Information

Video of FECO fringes and microscope images of 5CB in electric field. This material is available free of charge via the Internet at http://pubs.acs.org.

## AUTHOR INFORMATION

### Corresponding Author

*E-mail: jacob@engineering.ucsb.edu (J.N.I.).

### Notes

The authors declare no competing financial interest.

## ACKNOWLEDGMENTS

The research was primarily supported by the U.S. Department of Energy (DOE), Office of Science, Basic Energy Sciences (BES), under Award DE-FG02-87ER-45331: Kai Kristiansen (design of and experimental measurements with 3D force sensor and electric fields, analysis of optical microscope images; wrote paper with input from all coauthors); Jacob Israelachvili (experimental overview, design and fabrication of 3D force





DOI: 10.1021/acs.langmuir.5b00144
*Langmuir* 2015, 31, 3965−3972

sensor, interpretation of results). Hongbo Zeng (experimental design and execution of electric fields and optical microscopy, analysis of optical FECO fringes) acknowledges the support from the Natural Sciences and Engineering Research Council of Canada (NSERC). Bruno Zappone participated in the analysis of FECO fringes and interpretation of results.

## REFERENCES

(1) Blinov, L. M. Behavior of Liquid Crystals in Electric and Magnetic Fields. In *Physical Properties of Liquid Crystals*; Demus, D., Goodby, J. W., Gray, G. W., Speiss, H.-W., Vill, V., Eds.; Wiley: New York, 1999; pp 375−432.

(2) Li, Q. *Liquid Crystals Beyond Displays - Chemistry, Physics, and Applications*; Wiley: New York, 2012.

(3) Min, Y. K.; Hiramatsu, H.; Hamaguchi, H. Infrared Electro-absorption Spectroscopic Study of Association Structures of 5CB in the Solution, Isotropic Liquid and Nematic Liquid Crystal States. *Chem. Lett.* **2002**, No. 1, 68−69.

(4) Williams, R. Liquid Crystals in an Electric Field. *Nature* **1963**, *199* (489), 273−274.

(5) de Gennes, P. G.; Prost, J. *The Physics of Liquid Crystals*, 2nd ed.; Oxford University Press: New York, 1993.

(6) Gebbie, M. A.; Valtiner, M.; Banquy, X.; Fox, E. T.; Henderson, W. A.; Israelachvili, J. N. Ionic Liquids Behave as Dilute Electrolyte Solutions. *Proc. Natl. Acad. Sci. U. S. A.* **2013**, *110* (24), 9674−9679.

(7) Zappone, B.; Richetti, P.; Barberi, R.; Bartolino, R.; Nguyen, H. T. Forces in Nematic Liquid Crystals Constrained to the Nanometer Scale under Hybrid Anchoring Conditions. *Phys. Rev. E* **2005**, *71* (4), 041703.

(8) Kocevar, K.; Musevic, I. Observation of an Electrostatic Force between Charged Surfaces in Liquid Crystals. *Phys. Rev. E* **2002**, *65*, 030703.

(9) Zhang, X. J.; Zhang, X. H.; Xiong, Y.; Tian, Y.; Wen, S. Z. Anti-electroviscous Effect of Near-Surface 5CB Liquid Crystal and Its Boundary Lubrication Property. *Rheol. Acta* **2012**, *51* (3), 267−277.

(10) Haller, I. Elastic-Constants of Nematic Liquid Crystalline Phase of Para "Methoxybenzylidene-p-N-Butylaniline (MBBA)". *J. Chem. Phys.* **1972**, *57* (4), 1400−1405.

(11) Horn, R. G. Refractive-Indexes and Order Parameters of 2 Liquid-Crystals. *J. Phys. (Paris)* **1978**, *39* (1), 105−109.

(12) Kezdzierski, J.; Raszewski, Z.; Nowinowski-Kruszelnicki, E.; Kojdecki, M. A.; Piecek, W.; Perkowski, P.; Miszczyk, E. Composite Method for Measurement of Splay, Twist and Bend Nematic Elastic Constants by Use of Single Special In-Plane-Switched Cell. *Mol. Cryst. Liq. Cryst.* **2011**, *544*, 57−68.

(13) Faetti, S.; Gatti, M.; Palleschi, V. Measurements of Surface Elastic Torques in Liquid-Crystals - a Method to Measure Elastic-Constants and Anchoring Energies. *Rev. Phys. Appl.* **1986**, *21* (7), 451−461.

(14) Israelachvili, J.; Min, Y.; Akbulut, M.; Alig, A.; Carver, G.; Greene, W.; Kristiansen, K.; Meyer, E.; Pesika, N.; Rosenberg, K.; Zeng, H. Recent Advances in the Surface Forces Apparatus (SFA) Technique. *Rep. Prog. Phys.* **2010**, *73* (3), 036601.

(15) Ruths, M.; Zappone, B. Direct Nanomechanical Measurement of an Anchoring Transition in a Nematic Liquid Crystal Subject to Hybrid Anchoring Conditions. *Langmuir* **2012**, *28* (22), 8371−8383.

(16) Zeng, H.; Tian, Y.; Anderson, T. H.; Tirrell, M.; Israelachvili, J. N. New SFA Techniques for Studying Surface Forces and Thin Film Patterns Induced by Electric Fields. *Langmuir* **2008**, *24* (4), 1173−1182.

(17) Bradshaw, M. J.; Raynes, E. P.; Bunning, J. D.; Faber, T. E. The Frank Constants of Some Nematic Liquid-Crystals. *J. Phys. (Paris)* **1985**, *46* (9), 1513−1520.

(18) Ratna, B. R.; Shashidhar, R. Dielectric Properties of 4′-Normal-Alkyl-4-Cyanobiphenyls in Their Nematic Phases. *Pramana* **1976**, *6* (5), 278−283.

(19) Blinov, L. M.; Chigrinov, V. G. *Electrooptic Effects in Liquid Crystal Materials*; Springer-Verlag: Berlin, 1996.

(20) Crowley, J. M. In *Simple Expressions for Force and Capacitance for a Conductive Sphere near a Conductive Wall*; Proc. EAS Annual Meeting on Electrostatics, Electrostatic Society of America, 2008; p D1.

(21) Teixeira, P. I. C.; Sluckin, T. J. Microscopic Theory of Anchoring Transitions at the Surfaces of Pure Liquid-Crystals and Their Mixtures. 2. The Effect of Surface-Adsorption. *J. Chem. Phys.* **1992**, *97* (2), 1510−1519.

(22) Stannett, A. W. The Conductivity of Hydrocarbon Transformer Oil Containing Water and Solid Conducting Particles. *Br. J. Appl. Phys.* **1951**, *2* (Apr), 110−114.

(23) Pagliusi, P.; Zappone, B.; Cipparrone, G.; Barbero, G. Molecular Reorientation Dynamics Due to Direct Current Voltage-Induced Ion Redistribution in Undoped Nematic Planar Cell. *J. Appl. Phys.* **2004**, *96* (1), 218−223.





DOI: 10.1021/acs.langmuir.5b00144
*Langmuir* 2015, 31, 3965−3972